# Finishing of polycrystalline diamond tools by combining laser ablation with grinding

Christian Brecher[1,2], Fritz Klocke[1,2], Florestan Schindler[1], Andreas Janssen[2], Bettina Fischer[2], Jan-Patrick Hermani[2]

[1] *Laboratory for Machine Tools and Production Engineering (WZL) of RWTH Aachen University, Steinbachstr. 19, D-52074 Aachen*

[2] *Fraunhofer Institute for Production Technology IPT, Steinbachstr. 17, D-52074 Aachen*

Corresponding author: Florestan Schindler, Steinbachstr. 19, D- 52074 Aachen
f.schindler@wzl.rwth-aachen.de,
phone: +49 241 80 20393, fax: +49 241 80 22293

The project is being funded within the framework of the Federal Ministry of Education and Research, program VIP

Abstract:

In manufacturing PCD-tools, the finishing process in order to obtain the required surface and edge quality and to remove the damaged PCD layer induced by the prior manufacturing steps is mostly done by grinding. However, grinding is currently inefficient and costly due to low material removal rates and high wear of the grinding wheel. The project “Pro-PKD” aims to increase throughput and reduce tool wear by an additional laser ablation step prior to grinding. In first process investigations, the influence of different laser parameters on the ablation rate was analyzed and an optimum parameter set for maximum ablation efficiency was found. By measuring the overall material removal from the grinding wheel and the PCD tool, it could be shown that the G-ratio can be increased by at least a factor of two. Furthermore, the time required for grinding can be significantly shortened. As the time needed for laser ablation is only several seconds, in this way the whole time required for the finishing process can be reduced. In any case, the combined process presented here has the distinct advantage that it can be implemented into already existing grinding machines with comparatively low investment costs.

*Keywords: Grinding, laser ablation, polycrystalline diamond, combination process, tool wear*

# Laser ablation of polycrystalline diamond

## Introduction

Being one of the hardest and most wear resistant synthetic materials, polycrystalline diamond (PCD) has become an indispensable tool material for a wide range of applications. It allows the efficient machining of light metals, such as aluminum and magnesium alloys, or non-metallic materials like ceramics or composites with main applications in aerospace and automobile industry [1], [2].

PCD is composed of randomly oriented diamond grains in a metal matrix, which mostly consists of cobalt. Direct connections between the diamond grains significantly contribute to the toughness of the material [3]. PCD is produced in a liquid-phase sintering process, mostly as a 0.5-0.7 mm thick layer on a carbide holder. For the manufacturing of cutting tools, such PCD blades are diced into pieces mostly by either EDM [4] or laser cutting [5]. All dicing methods lead to a rather low surface quality and a damage of the surface near zone, which reduces tool life. Therefore, a finishing process is required to create high-quality cutting tools. The most widely used method for finishing is grinding, which provides a high surface quality and long tool lifetime. However, due to its high hardness, PCD can only be ground by diamond grinding wheels [4]. The low material removal rate and high tool wear make this process an important cost factor in PCD tool manufacturing. Finishing by laser ablation is also possible but generally leads to a lower surface quality and reduced tool life compared to grinding [personal correspondence]. Therefore, laser machining is currently mainly used for cutting and the generation of chip breakers.

In this paper, a novel finishing method for PCD cutting tools, which is based on the combination of laser processing and grinding, is presented. Laser ablation is used to either completely or partially damage or remove the surface layer of the cutting edge, which was influenced by the dicing process. A high surface quality is achieved by subsequent grinding. By this combination process, the total time required for finishing as well as the wear of the grinding wheel shall be reduced.

This paper deals with first experimental results on the process combination. First, experiments on laser ablation and the optimisation of processing parameters are presented. Next, the following grinding process is explained. Afterwards, studies about the influence of laser ablation on the grinding process are shown and discussed. The obtained results demonstrate that the combination process allows to significantly reduce the time required for finishing as well as the grinding tool wear. Therefore, it has a high potential to make the finishing process more efficient and significantly lower manufacturing costs.

## Ablation mechanisms

Commonly, laser ablation is conducted using pulsed laser radiation. The ablation process is characterized by transition of irradiated material from solid to liquid and vapor. The phase transitions occur consecutively induced by conversion of radiation energy into thermal energy within the material, which means the transmission of photon energy from the absorbing electrons to the lattice. The pulse width $t_p$ mainly determines the physical characteristic of the ablation process. For pulse width $t_H > 1$ ns (= $10^{-9}$ s), the process is called *short pulse (SP)* laser ablation and is characterized by a significant amount of material being removed from the irradiated area in liquid phase by the pressure of the evaporating material. Essential for this process is the high absorption of laser energy in the evaporated material within the duration of one laser pulse. Since the phonon thermalization process within the material happens within several ten picoseconds (1 ps = $10^{-12}$ s), in the case of so called *ultra-short pulsed (USP)* laser radiation, the heating takes place mainly after the pulse duration. Thus, the material removal occurs mainly by evaporation. [6]

## Experimental setup and methodology

From a production technological point of view, the main characteristic of short pulse laser ablation is a high ablation rate per pulse accompanied by large amounts of ejected melt. Ultra-short pulse laser ablation exhibits higher accuracy and almost no melt ejection at the cost of low ablation rates per pulse. Since in this work structures in PCD material are generated aiming for weakening the bulk material, the technological advantages of ultra-short pulse laser ablation are not prior for this purpose. Therefore, USP laser ablation will be used in the project

mainly for investigating the influence of ablated structures on the bulk resistance excluding thermal modification of the surrounding PCD material. In the present paper only nanosecond laser ablation is analyzed.

A laser ablation system was utilized containing a nanosecond laser emitting linearly polarized radiation at 1064 nm wavelength. The entire system was installed at *Fraunhofer IPT* by implementing the laser source (EdgeWave IS4I-E) into a common 5-axes milling machine. The optical setup contains a dynamic beam expander and a galvanometer mirror scanner for z and x-y movement of the laser beam as well as a telecentric f-theta lens with a focal length of 163 mm. Table 1 shows the main specifications of the utilized laser source. Although the parameter studies were executed in terms of a 2,5 D-surface structuring on flat samples, the system can also be utilized for the 3D-treatment of complex formed cutting inserts.

| | |
|---|---|
| laser type: | Nd-$YVO_4$ |
| mode of operation | pulsed & cw |
| wavelength: | 1064 nm |
| pulse width: | 6 ns to 34 ns |
| maximum output power: | 38 W |
| maximum pulse energy: | 3,43 mJ |
| pulse repetition rate: | 5 kHz to 40 kHz |

**Table 1: Specifications of the ns laser source [EdgeWave]**

The focal diameter in this configuration is 24.6 µm, according to Figure 1, where an elliptic spot is determined via the x- and y-radius. Thus, the maximum fluence at 3,43 mJ pulse energy is around 180 J/cm². However, the fluence is independent from the pulse duration, which plays a crucial role for the ablation process. Thus it only offers significant information for constant irradiation durations. A characteristic of the utilized laser source is pulse width change with varying repetition rates and output power. For a reasonable discussion of ablation results the applied fluence have been calculated based on given pulse energies at the different operation conditions. In the future works within the project, laser pulse lengths will be varied systematically. Thus, the influence of varying pulse durations at constant fluence on the ablation result will be analysed . Since this

correlation is not revealed at this time, the ablation results in the present work are correlated to the fluence, neglecting the influence of irradiation duration.

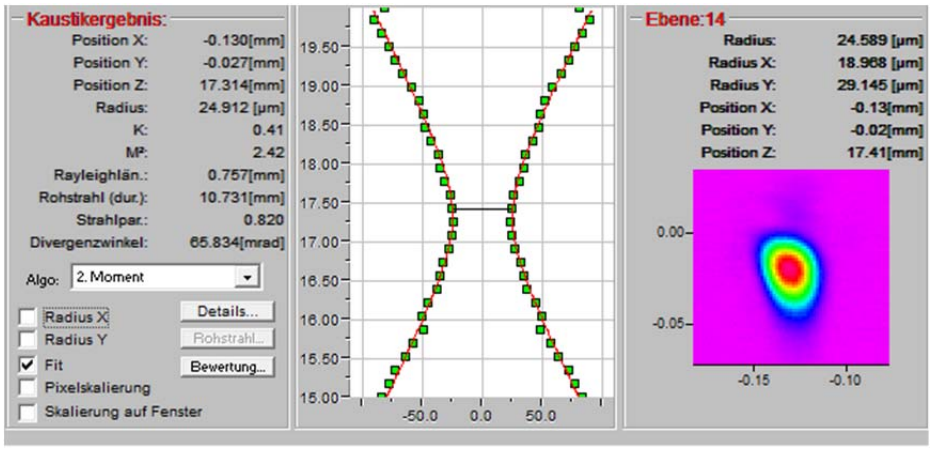


**Figure 1: Laser beam measurement at 5 kHz, 100 % Power**

According to the manufacturing history of the cutting inserts, the thickness of the layer to be removed is up to approximately 40 µm. Therefore, laser ablation is considered to reach a depth of about 35 µm. Parameter studies were conducted in order to obtain the correlation between the mainly relevant process parameters and the resulting ablation rate. According to the German standard DIN 32540, parameters to be studied were defined as:

- Pulse repetition rate $f_{rep}$: defines the pulse period $t_p$
- Pulse overlap PO
- Pulse duration $t_H$
- Fluence F, defines the single laser pulse energy per irradiated area [$J \cdot cm^{-2}$]
- Intensity I, defines the single laser pulse energy per irradiated area and time [$J \cdot s^{-1} \cdot cm^{-2}$]
- Defocusing $\Delta z$, defined as the distance between the focal area and the working distance

## Results of the laser parameter study

In order to get detailed information on the ablation process, first experiments investigating the ablation effect of single pulses were carried out. Main goal of these tests was to observe the material response on single pulse irradiation with varying laser pulse parameters.

For these experiments, pulse repetition rate and laser beam feed rate were aligned in a way that punctiform single pulse ablation structures (*dimples*) were spatially separated, as illustrated in Figure 2. If the feed rate is selected to be high enough, the ablation dimples are well separated by a distance Δx (eq.1) leading to punctiform ablation structures.

$$\Delta x = \frac{v_f}{f_{rep}} \qquad (1)$$

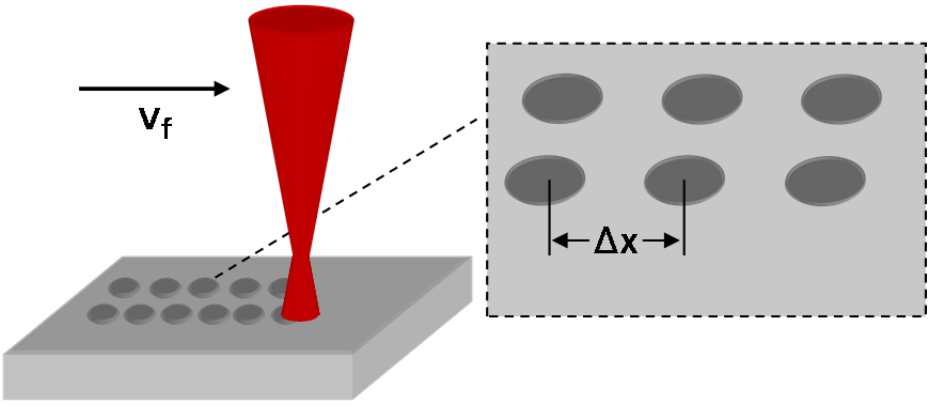


**Figure 2: Illustration scheme of single pulse separation**

Figure 3~~Figure 3~~ shows the resulting ablation depth of punctiform ablation structures created with multiple irradiations according to Figure 2. The experiments were conducted at 5 kHz with a pulse width of 7 ± 1 ns. An almost linear relationship between applied fluence and the absolute ablation depth is apparent, which is plausible since no interaction between subsequent laser pulses occurs. A total depth of 25 µm could be reached within 50 repetitions of single pulse superposition, indicating an ablation depth of 2 µm per pulse.

Punctiform ablation structures *(dimples)* are not foreseen for grinding investigations in this project since they would cause higher overall process times than manufacturing continuous structures like grooves, lattice structures or planar indentations. But the achieved results serve as basis for designing ablation strategies in order to – meeting the production demands – achieve maximum material removal in minimum time. The demand for high ablation efficiency is also the reason, why laser powers lower than the ones shown in Figure 3 have not been investigated.

The results concerning single punctiform ablation structures were used to design strategies for generating the targeted structures – grooves and plane ablation. Ablation structures in terms of straight lines were generated by applying a linear motion of the laser beam over the target surface. Adjusting pulse repetition rate and laser beam feed rate, single laser pulses, each removing a cone-shaped punctiform ablation geometry, are superposed with defined overlap. Although ablation accuracy is not a prior demand in this investigation, the ablation depth must be controlled rather accurately. Since the objective of the process combination is to minimize the necessary grinding effort, large deviations in the laser affected layer depth can cause remaining thermal stresses in the cutting tool surface after grinding.

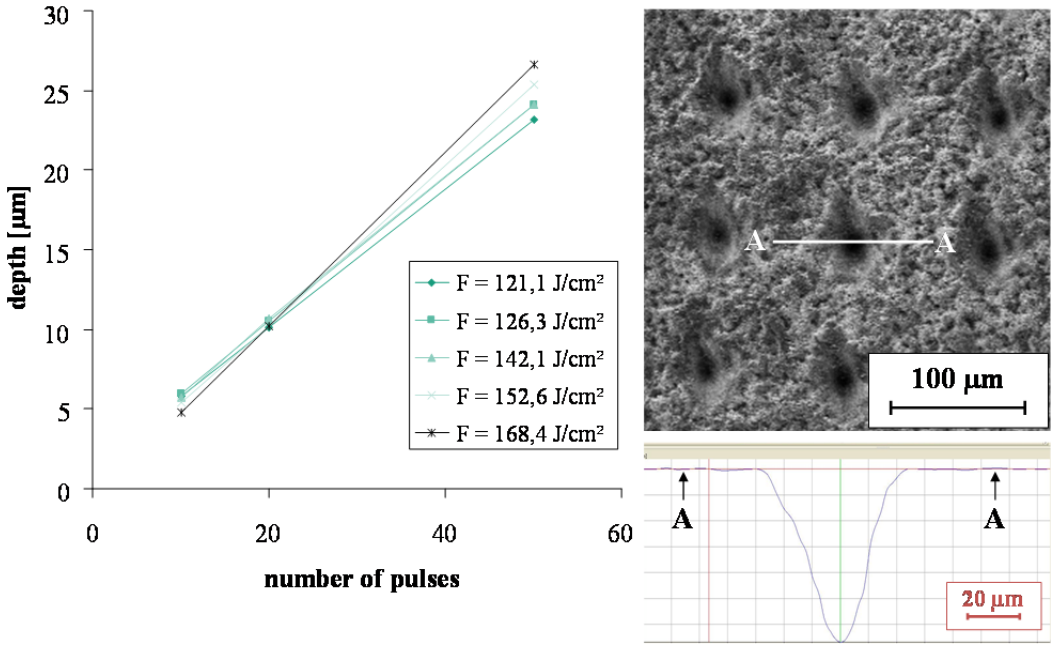


**Figure 3: Dependence of the ablation depth on the number of irradiations paths for several values of the laser power (left) and SEM image of a multi pulse cone with depth measurement (right). Each measurement point was achieved by measuring 3 single dimples and calculating the mean value. The deviation of the points amounts to around 0.1 µm each, thus due to the scale of the diagram, the deviation is not depictured.**

By adjusting the pulse overlap, the residual z-profile in the ablation ground has been smoothened. Instead of calculating the pulse overlap PO, the absolute distance Δx between two subsequent laser pulses has been determined according to eq. (1), with $v_f$ being the lateral laser beam feed rate.

Figure 4 shows resulting profiles of grooves formed with a pulse distance of 20 µm (left) and 10 µm (right) using 10 cycles of irradiation. While the height

profile in the left example amounts to Rz > 2.0 µm, it could be reduced to Rz < 0.5 µm using an adequate pulse distance.

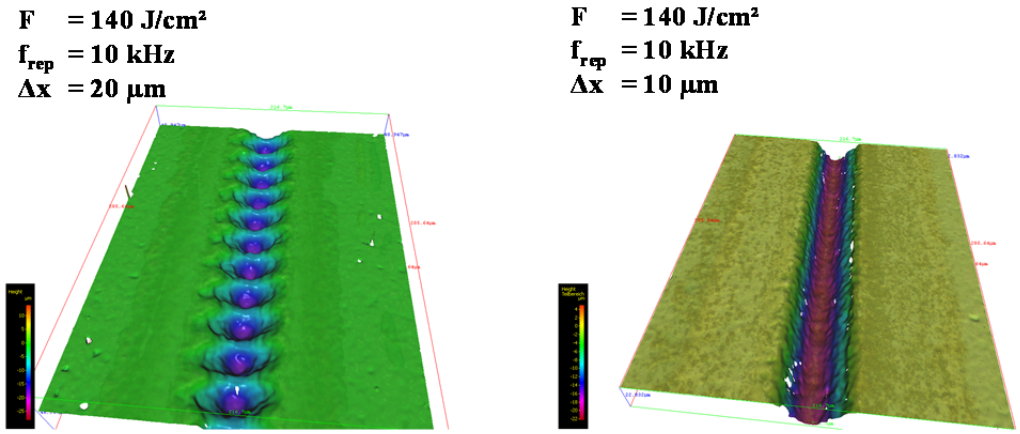


**Figure 4: Influence of pulse distance on groove profile**

With the given process parameters, the overall manufacturing time for a milling insert, as used in this project, can be estimated. The target ablation depth is 35 µm. Presupposed an area to be laser treated of 4.5 mm x 0.5 mm, the pure laser ablation time can be limited to 10 seconds.

At this point it can be noted, that within the investigation of the structures on the PCD work piece no debris due to melt expulsion – which is typical for short pulse laser ablation – has been found. This has been observed first on grooves and was proved for plane ablation (Figure 5~~Figure 5~~, Figure 9~~Figure 10~~) using the same process parameters: $P_L$ = 100%, $f_{rep}$ = 10 kHz, Δx = Δy = 10 µm.

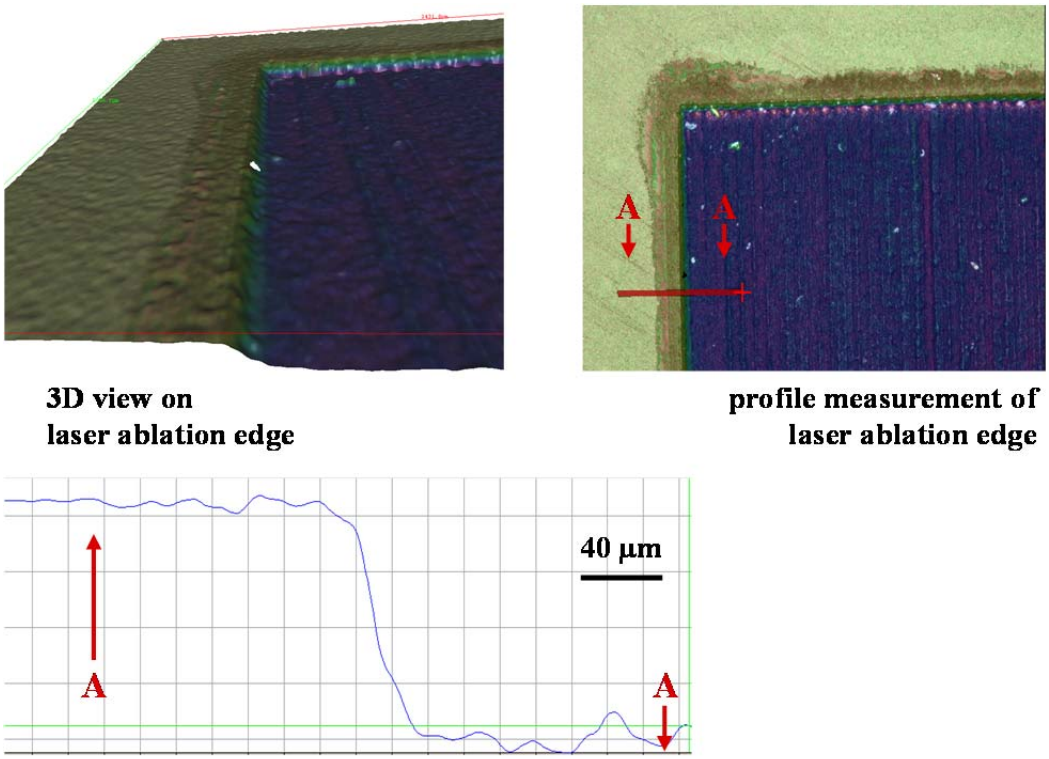


**Figure 5: SP laser ablation edge showing no burr due to melt expulsion during irradiation**

In order to increase the ablation efficiency, experiments were conducted containing a variation of the working distance. Since the focused laser beam is divergent leaving the focal range, a widening of the irradiated area causes an increase of the irradiated work piece area. Two phenomena can occur: If the fluence in the focal range is in the vicinity of the ablation threshold of the work piece, the defocusing will cause a broadening of the ablation geometry accompanied with a decrease of the resulting depth. In the second case, the pulse fluence in the focal range is significantly higher than the ablation threshold, causing plasma shielding and thus a limitation of the ablation efficiency – a huge part of the incoming radiation is absorbed within the plasma [6, p.3]. Hence, a broadening of the irradiated area can enhance the absolute energy absorption.

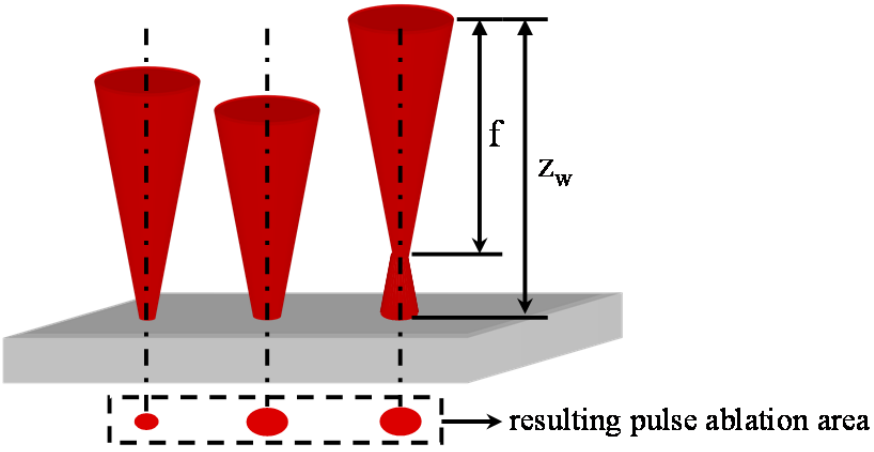


**Figure 6: Influence of working distance on irradiated area**

The correlation between defocussing and resulting irradiation area can be obtained by Figure 1. Such measurements can be used to determine focal diameters either directly from the data or, in case the defocussing exceeds the range of beam profile measurement, by interpolation. Figure 7~~Figure 8~~ shows the dependence of the ablation depth on defocusing in positive and negative z direction. The asymmetric appearance of the graph arises from an asymmetric intensity profile of the laser source outside the focal range. Nevertheless, an increase of the ablation depth by 25% can be obtained positioning the focal point 750 µm beneath the work piece surface.

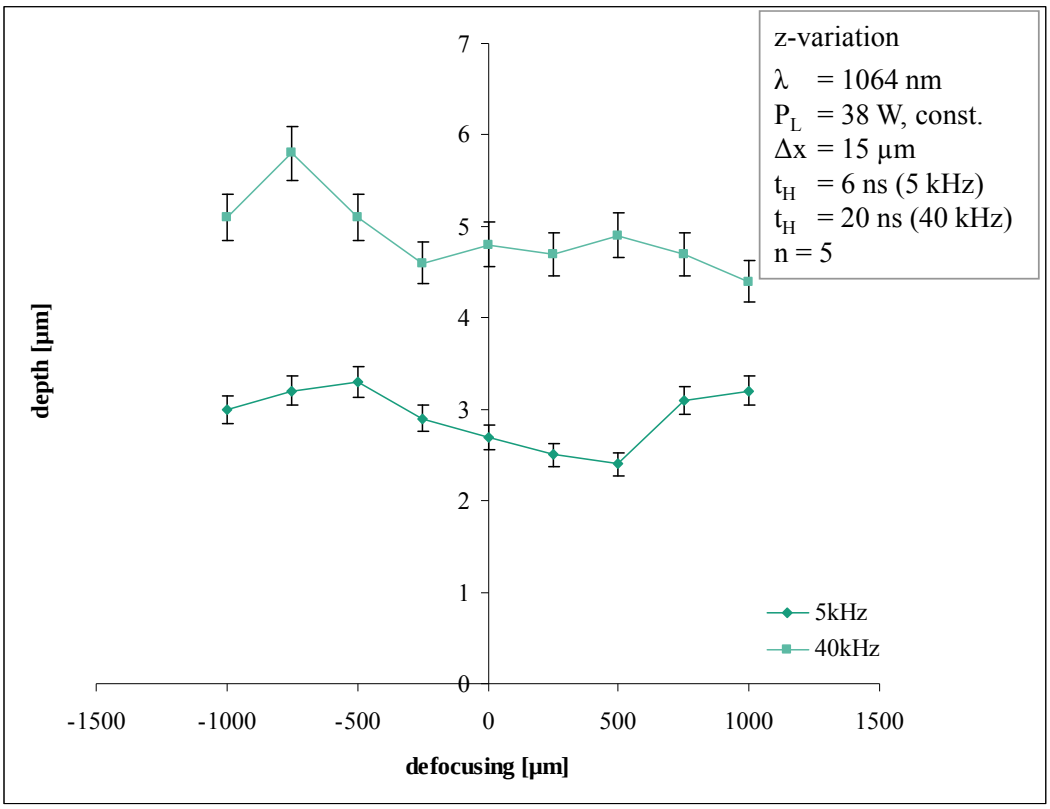


**Figure 7: Influence of defocusing on ablation depth, mean values with std. var.**

These experiments were conducted with maximum laser power applying five repetitions, which means five cycles of irradiation. Using these results for adapting the process strategy for manufacturing the desired grooves of 35 µm depth into cutting inserts (see Figure 8~~Figure 9~~), the overall laser ablation time could be reduced to 7 seconds. In Figure 7, a groove on the PCD substrate after laser treatment was analyzed with a focused ion beam microscope (FIB). This preparation method uses gallium $Ga^+$ ions which are accelerated towards the PCD substrate and remove PCD material without damaging its vicinity. The lateral faces of the generated craters can be analyzed directly within the microscope or subsequently with a scanning electron microscope (SEM). The lateral sides of the groove were covered with vaporized material from the ablation process. The cross-section shows no cracks within the zone underneath the bottom of the groove, this means the laser irradiation does not seem to significantly influence the remaining PCD material. Further investigations by transmission electron microscopy will reveal whether there are changes of the material structure or composition, which could not be observed so far.

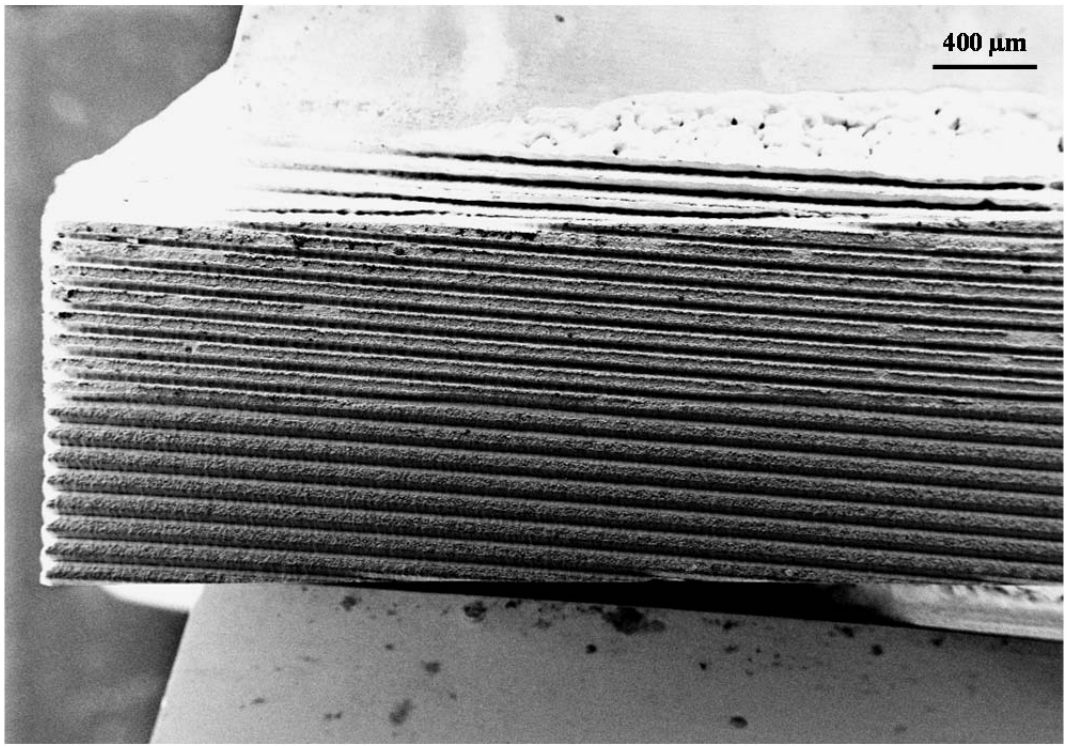


**Figure 8: Cutting insert with SP laser ablated grooves**

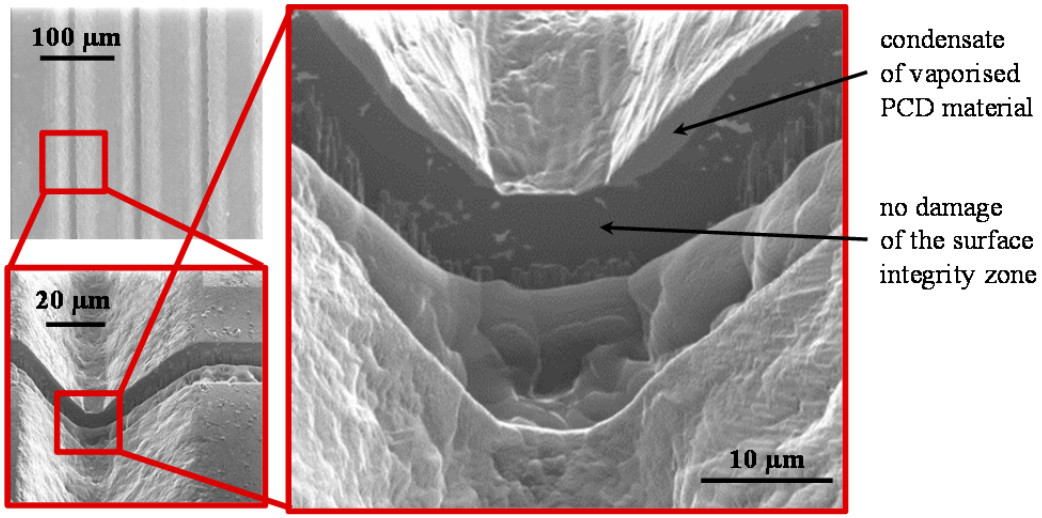


**Figure 9: FIB analysis of a laser groove on a PCD sample**

A magnification of the edge of the laser ablated groove (Figure 9~~Figure 10~~) shows that no ablation product, such as remelted and expelled material, is apparent.

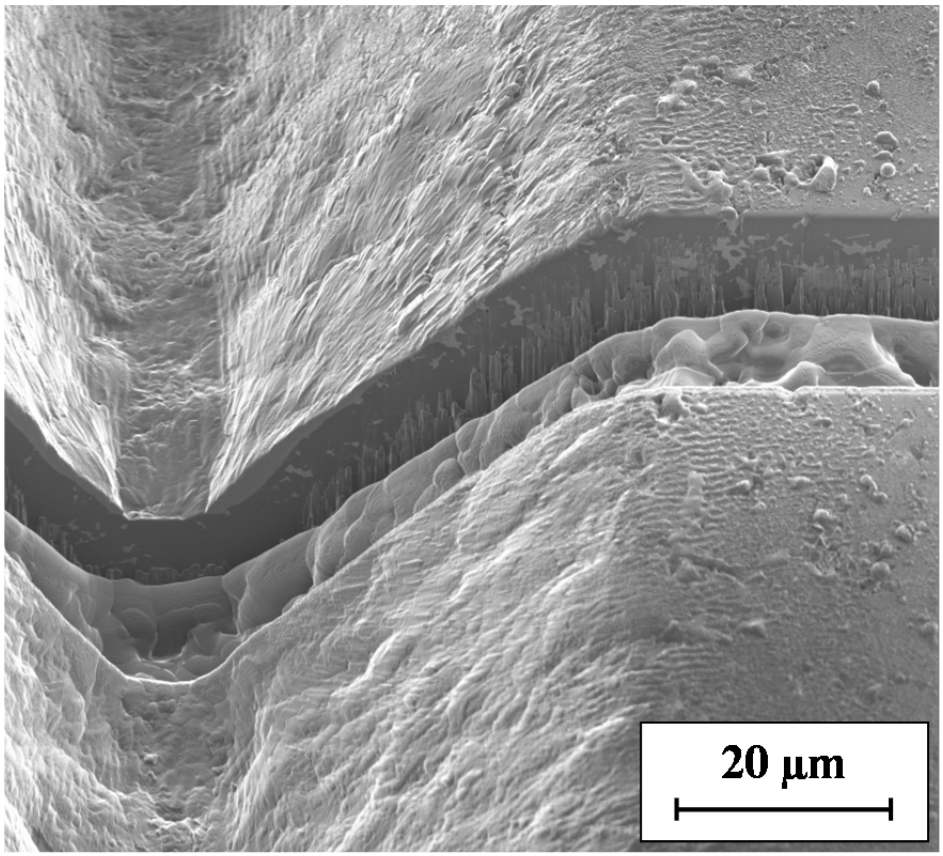


**Figure 10: SEM image of a laser ablated groove with ion beam cut area**

## Grinding of PCD

The decisive material properties of polycrystalline diamond PCD as a high performance cutting material implicate difficulties in the machining of PCD tools. This means in terms of grinding a challenge for the process control, for the grinding machine and for the grinding wheels. The Knoop hardness of PCD is given with 50 GPa and thereby reaches almost the range of diamond with 57 – 104 GPa, but as an advantage for some applications it is isotropic as a result from the sintering process [10]. The grinding process of hard and brittle materials, which is mostly machined with diamond wheels, can be characterized by low material removal rates and extremely high values for the grinding wheel wear [11]. Industrial applications address values between G = 0.01 – 0.05 for the grinding ratio [12, 13]. Current studies might have found an explanation for the material removal behavior in machining diamond with diamond edges, where process loads lead to the formation of an amorphous layer with an in-process growth rate that correlates with experimental wear rates [14]. However, the comparison of the content of diamond grains of the engaging diamond wheel and the PCD substrate reveals the big differences in toughness, fracture resistance and

hardness. PCD consists to at least 90 vol.-% of diamond grains, according to PCD type average grain size of 2 µm - 25 µm, whereas state-of-the-art grinding wheels are composed of approximately 25 vol.-% to 30 vol.-% diamond with a mean grain size of 15 - 25 µm and hybrid bond types which represent a mixture between vitrified and resin bonds. The machinability of this brittle material is significantly different from machining ductile materials in terms of a material removal by means of micro crack formation and resultant fragment breakaway [10, 15]. To meet the requirements of fracture toughness, PCD is sintered with carbide material, otherwise the edges would brake prematurely due to brittleness.

## Experimental setup for PCD grinding

The grinding experiments were conducted at the *Laboratory for Machine Tools and Production Engineering WZL* on a five axes tool grinding machine S22P Turbo, *Feinmechanik Michael Deckel GmbH*, which operates with three translational and two rotary axes for the grinding spindle ($P_{max}$ = 15kW) and the work piece clamping (machine kinematics in Figure 8, bottom right). In order to ensure a firm and vibration resistant hold of the inserts, an apparatus has been developed which consists of a SK50 mandrel, a multicomponent dynamometer and an insert holder type D 45° (Figure 11, left). The force measurement device is composed of four three-component-force-sensors. The construction allows the grinding of both tool flanks and the tool face at one clamping position.

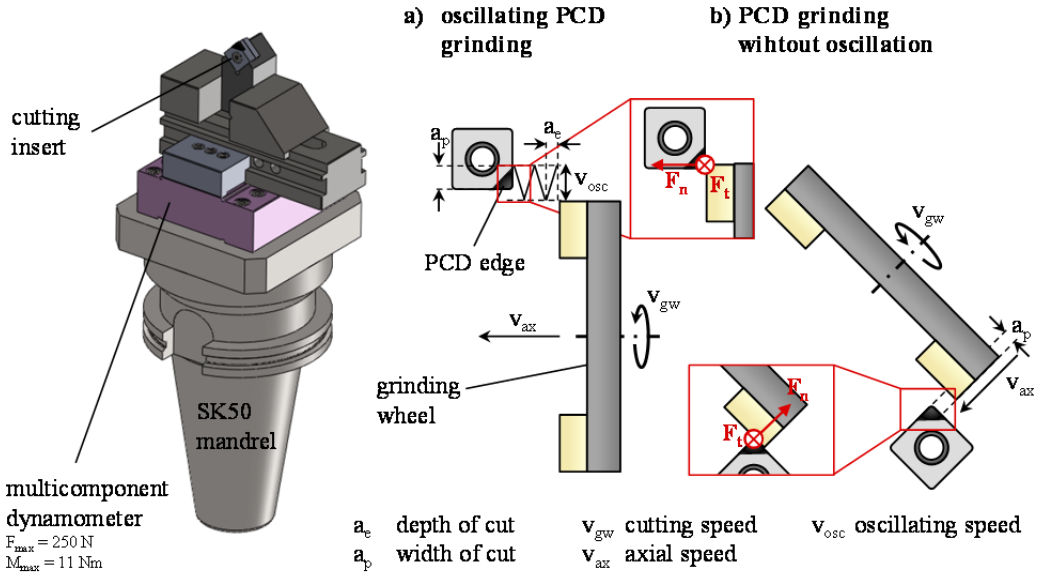


**Figure 11: Machine setup and process control**

The preliminary grinding tests have been carried out in order to deduce a basic process knowledge from industry oriented PCD grinding. The tool path is given in Figure 11a. All tests were carried out with a diamond cup wheel, D 20 µm average grain size, with hybrid bond. The dressing was carried out with a rotating silicon carbide dressing tool. Coolant oil was applied via several solid nozzles. The diamond cup wheel grinds with its face side orthogonal towards the tool flank with an infeed speed $v_{ax}$ while oscillating over the width $a_p$ of the insert (no clearance angle, a lateral view is given in Figure 12 top right). The oscillation of the grinding wheel generates an even axial wheel wear and thus facilitates a precise machining.

Currently, grinding of PCD with force control has turned out to be a good procedure in dominating the process loads and the wheel wear. Nevertheless, all experiments were conducted without force control but with force measurement. From measuring the process forces the process loads and vibrations and thus changes of material removal behavior and occurring wear on the grinding wheel can be derived.

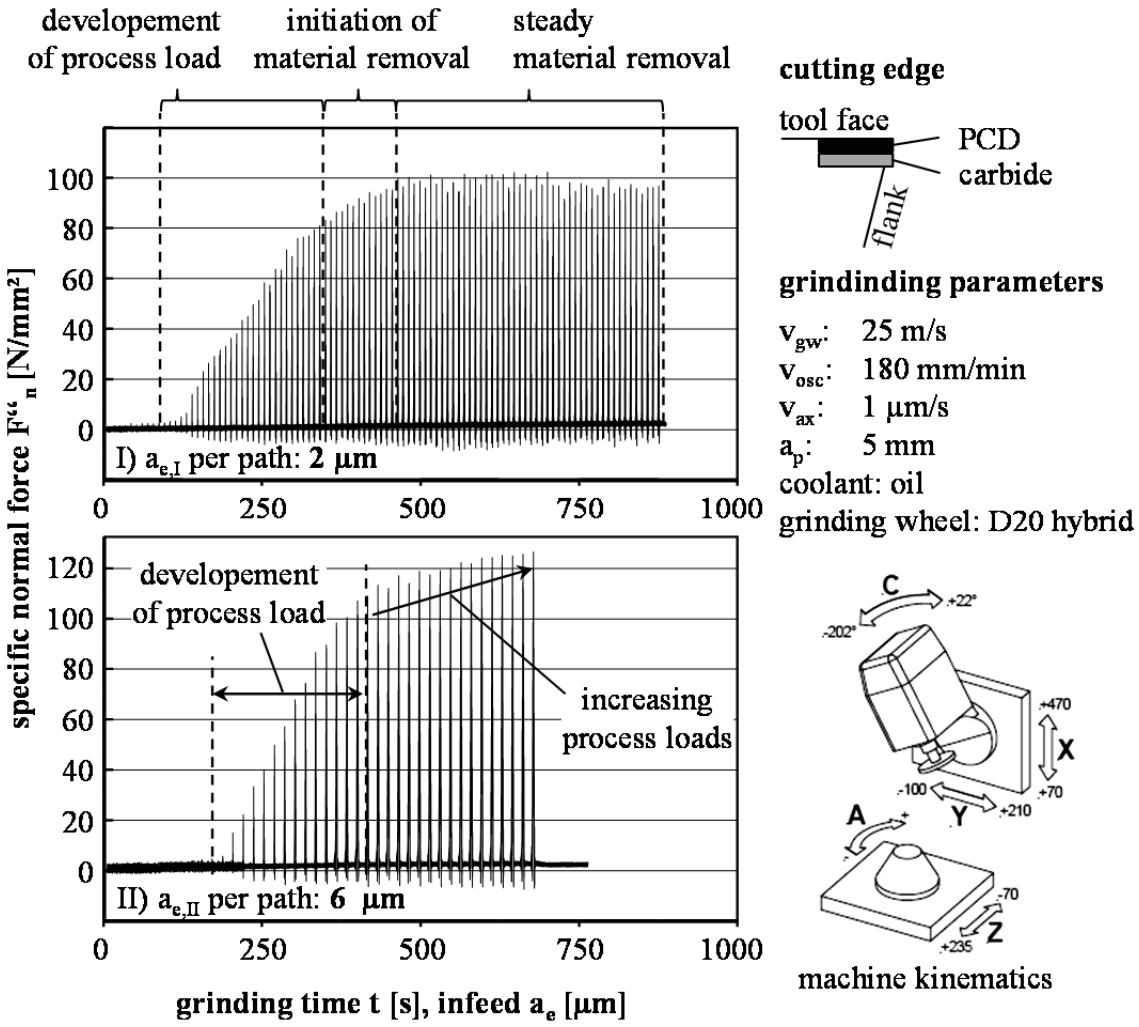


**Figure 12: Specific normal force in oscillating grinding without force control**

The determination of the layer thickness of the PCD-inserts revealed a strong deviation of the thickness proportions between PCD layer and carbide layer, for instance the PCD layer thickness reaches from 433 µm to 642 µm even if the total thickness of the PCD tip was constantly determined with 988 ± 4 µm. Hence, the grinding forces were related to the ground area of PCD and thus represent the specific normal force F''n [N/mm²] and the specific tangential force F''t [N/mm²]. Figure 12 shows the curve progression of the specific normal forces in grinding of a PCD insert with oscillating process modification (a) (Figure 11a). During the grinding operation, all process parameters were kept stable except for the depth of cut per path $a_e$, which was increased from $a_{e,I}$ = 2 µm up to $a_{e,II}$ = 6 µm.

At the initiation contact of the diamond grains with the PCD substrate, a linear increase of the specific normal force could be observed. Subsequently, the force values rise until the minimum process load is exceeded and both material removal

and wheel wear start. This could be observed by a declining force trend. Depending on grinding wheel type, the machine rigidity and the grinding parameters, the process forces remain at a steady level when wheel wear and removed PCD volume stabilise (I). In case (II), the process forces lead to an overload of the grinding wheel. In this situation, the grains are not able to remove the fed PCD material and wear out preliminary. Furthermore, pore clogging with carbide material decreases grain protrusion as well as space for chips and coolant. Consequentially, lower material removal rates and higher process forces and temperatures occur.

For further investigations on grinding wheel wear and the grinding ratio, the process control (a) has been modified to process (b) for which grinding wheel oscillation was not executed. Based on the fact, that cutting speeds in tool grinding exceed the oscillation speed by a factor of several thousand, a comparison by means of grinding forces and wear behavior is scientifically reliable despite of no oscillation. The wheel wear was determined by grinding a wear plate.

In order to compare different grinding operations with respect to the influence of the laser treatment, the grinding process was set perpetually to modification (b), compare Figure 11b. For process modification (b), the width of cut was set to $a_p$ = 3 mm, the axial feed speed was constantly $v_{ax}$ = 1 µm/s and the cutting speed $v_c$ = 20 m/s. The grinding process was started with an approximate allowance of 50 µm. The grinding process was manually aborted 100 seconds after the first contact (force observation) between grinding wheel and work piece when a total depth of cut of $a_e$ = 100 µm was reached. For each strategy, three PCD inserts were ground successively.

### Combination of laser ablation and grinding

In order to investigate the influence of the laser treatment on the grinding process in machining PCD (mean grain size 10 µm), the volume of removed PCD material, the grinding wheel wear and the process forces were analyzed after grinding of three insert samples. The in-process grinding force development in modification (b) showed a similar behavior to modification (a) even if some

differences could be observed. Several force drop-offs are observed (labeled in Figure 13) during each grinding test, which could also been monitored by an acoustic emission sensor (bottom right). The force drop-offs do not reliably start at a specific process load nor end at steady minimum. However, the drop-offs take place within approximately 0.3 seconds and lead to an increase of the grinding force ratio μ. Some investigations, in which the grinding process has been stopped before (no drop-off) and after a maximal threshold of 60 N/mm² when a drop-off had occurred, showed no significant correlation between drop-off and removed PCD volume, hence it is assumed that it is a consequence of grinding wheel wear. In pretests the axial speed was varied from $v_{ax}$ = 0.1 μm/s to $v_{ax}$ = 6 μm/s, under each condition the force drop-offs had occurred as well. The grinding parameters and the developed grinding forces specific to the contact area of ground PCD were comparable to industrial values. However, due to the strong deviation of the force drop-offs, this could not be proven nor could the drop-offs be narrowed. So far this behavior is not investigated entirely and has to be analyzed within further investigations. Grinding of laser-structured PCD showed a smaller slope at the beginning and in addition to that less vibrations during the process. Considering the wear and material removal progress after grinding, an increase of the ratio of volume of removed work piece material to volume of abrasive wheel wear from G = 0,013 to G =0,024 could be observed. This was mainly influenced by a higher rate of removed PCD material, removed carbide material was not taken into account for the G-ratio. The analysis of the ground PCD surface after “laser treatment and grinding” and after “grinding without laser treatment” (Figure 14) on the tool flank showed no existence of any grooves or scratches from the grinding process (Ra = 0.05 – 0.09 μm, Rz = 0.31 – 0.58 μm on both samples), even no cracks or other influences of the integrity zone could be found after FIB analysis.

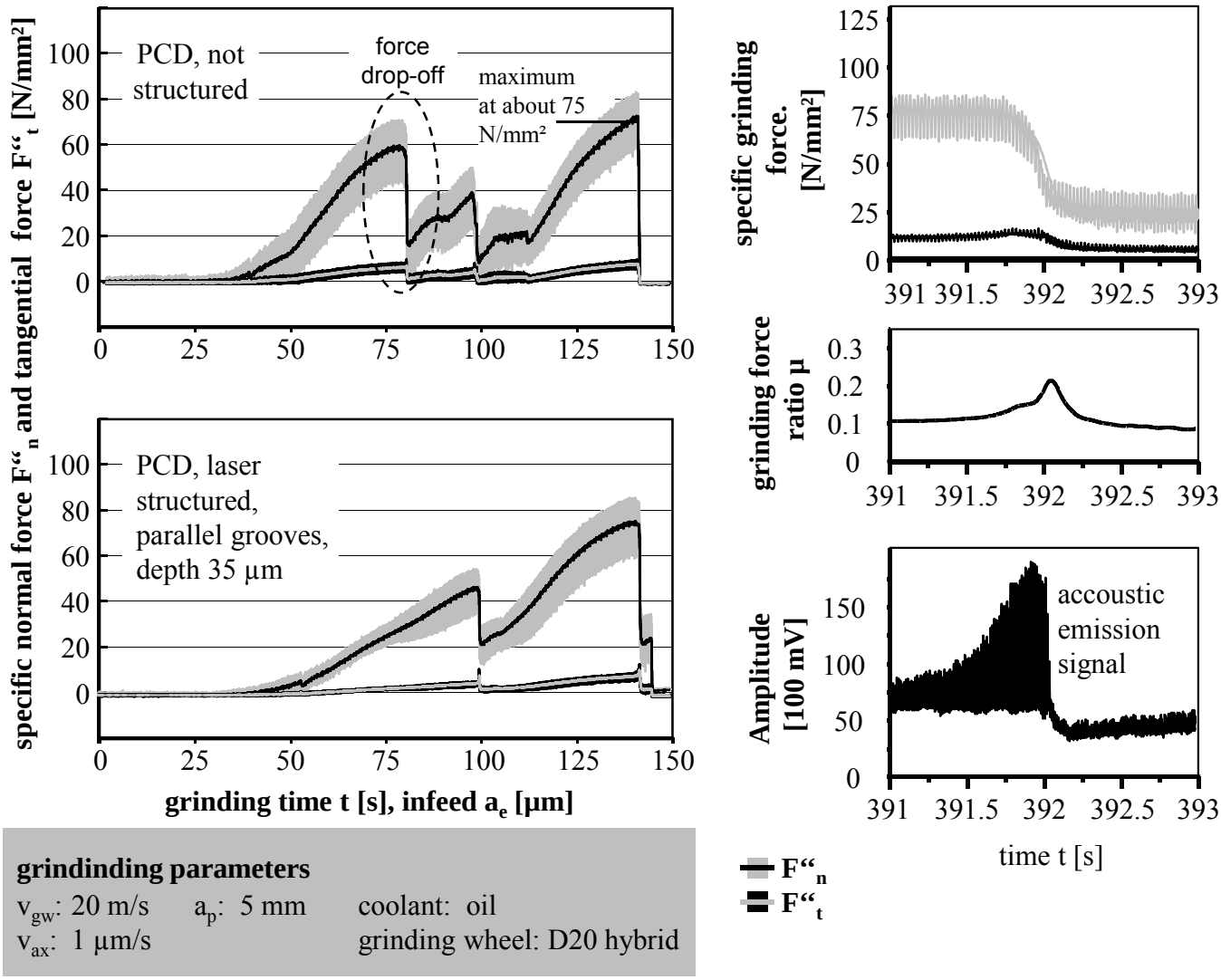


**Figure 13: Grinding force in machining of PCD and laser structured PCD**

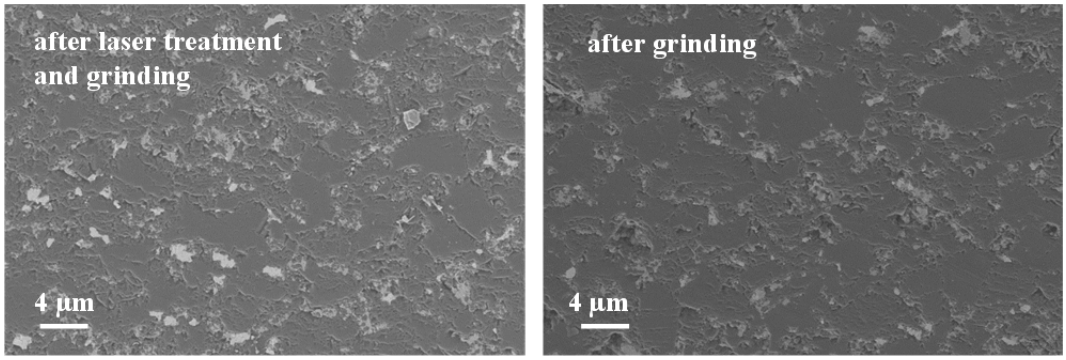


**Figure 14: SEM pictures of two PCD samples after grinding on the tool flank**

## Discussion

The obtained results indicate a special ablation behavior of PCD under ns-laser pulse irradiation as carried out here. As described above, PCD consists of approximately 10 µm sized diamond grains embedded into a cobalt matrix. The

direct band gap of diamond is 7.3 eV which is significantly higher than the laser photon energy of 1.17 eV at $\lambda = 1064$ nm. Thus, in the regime of linear absorption, which is dominant in SP laser ablation, diamond exhibits a high transmittance for the used wavelength of 1064 nm [7]. Hence, the major part of the impinging radiation should pass the diamond grains. As the individual diamond grains are surrounded by cobalt [8], it can be assumed that the absorption of laser radiation is alike absorption at a porous surface. As cobalt exhibits an absorbance of approx. 30 % [17], the main absorption is expected to occur in the cobalt matrix, in which the entire energy is deposited into a layer thickness of several nanometers. In this proposed model, a high absolute absorption is expected, since reflected laser radiation impinges on cobalt surfaces again, like radiation impinging on a sponge like surface.

Following [9], PCD with cobalt added as sintering aid is thermally instable. At temperatures above 875°C, diamond graphitizes in oxygen. Since cobalt acts as catalyst in this reaction, graphitization occurs at significant lower temperatures around 810°C in the presence of cobalt. It is assumed that the photon energy is absorbed in the cobalt matrix leading to a fast heating, melting and evaporation of the metal. Hence diamond is graphitized at the boundaries and heat is conducted in the bulk material, thus causing enhanced graphitization in the bulk. Graphite however has a very high absorptance slightly below 100%, which, taking also into account the very high heat conductivity of diamond, suggests an ablation process as follows for SP laser ablation of PCD:

1. Absorption of laser radiation at the first cobalt layer
2. Melting of cobalt
3. Heat transfer to diamond
4. Heating of diamond
5. Graphitization
6. Evaporation of cobalt inducing
    - removal of cobalt
    - damaging of diamond/graphite bulk
    - removal of graphite/diamond particles

This idea is similar to the suggestion Li et al. [7], [8] made for femtosecond laser ablation of PCD. In contrast to that model, for nanosecond pulses, the laser radiation is probably mainly absorbed by the cobalt matrix and heat conduction as well as bulk heating become more dominant [9].

## Summary and outlook

For manufacturing PCD-tools a finishing process is necessary in order to remove the damaged PCD layer induced by the prior manufacturing steps. Currently, grinding is the most widely used finishing process as it provides a high surface quality and tool life time. However, grinding is currently inefficient and costly due to the low ablation rate and high wear of the diamond grinding wheels. The project “Pro-PKD” aims to increase throughput and reduce tool wear by an additional laser ablation step prior to grinding.

For this purpose, two laser ablation strategies are investigated. The first one involves generating defined ablation geometries like notches or grids into the surface in order to enhance the notch effect for grinding. For the second one, the entire damaged surface layer is removed by the laser and grinding is used to smoothen the surface afterwards. The second strategy will be studied in further process investigations.

In first process investigations, the influence of different laser parameters on the ablation rate was analyzed and an optimum parameter set for maximum ablation efficiency was found. It was shown that for a slight defocusing of the laser spot on the work piece, plasma formation is reduced so that the supplied laser energy can be efficiently used for ablation. With the optimized parameter set, grooves of 35 µm depth with a distance of 100 µm could be applied to the whole PCD surface area of a cutting tool insert within 7 s.

For several PCD tools prepared with different laser ablation geometries, the processed surface layer was completely removed by subsequent grinding. The grinding forces were monitored throughout the entire process. The normal force was shown to exhibit a saw tooth profile, which was shown to originate from sudden removal of a significant amount of grinding wheel material. By measuring the overall material removal from the grinding wheel and the PCD tool, it could be shown that the G-ratio can be increased by at least a factor of two. In order to minimize the necessary grinding wheel operation, the entire damaged PCD

surface will be ablated, followed by grinding solely for smoothening the surface. Furthermore, the time required for grinding can be significantly shortened. As the time needed for laser ablation is only several seconds, in this way the whole time required for the finishing process can be reduced.

To get a comprehensive understanding, the suggested ablation process will be further analyzed. Experiments regarding the ablation mechanism for nanosecond pulses will be conducted to investigate in more detail the remaining surface conditions, surface near material properties and the ablation products. On this basis, the applicability of the ablation model for PCD under ns-pulse laser irradiation suggested above will be examined.

In further process investigations, the combination process will be further optimized and analyzed. To validate the feasibility for industrial use and the economic efficiency, tool life tests will be carried out. Here, a comparison of tool life with the conventional grinding process is necessary to ensure that the laser process does not reduce the tool quality. Furthermore, comparisons with the recently emerging processing by ultra-short pulsed lasers will be carried out. In [18], it was shown that for processing of composites, PCD tools manufactured in this way have a tool life comparable to conventionally ground ones. However, the tool life for processing harder materials like carbide or titanium has not been investigated so far.

In any case, the combined process presented here has the distinct advantage that it can be implemented into already existing grinding machines with comparatively low investment costs.

# References


[1] Abele, E.; Schramm, B. (2008) Using PCD for machining CGI with $CO_2$ coolant system; Production Engineering Research and Development, Vol. 2

[2] Heath, P.J. (2011) Developments in applications of PCD tooling. Journal of Material Processing Technology 116: 31-38

[3] Lammer, A. (1988) Mechanical properties of polycrystalline diamonds. Materials Science and Technology 4: 949-955

[4] Tso, PL, Liu, YG (2002) Study on PCD machining. International Journal of Machine Tools & Manufacture 42: 331–334

[5] Zhang GF et al. (2007) An Experimental Study on Laser Cutting Mechanisms of Polycrystalline Diamond Compacts 56: 201-204

[6] Poprawe, R. (2011) Tailored Light 2 – Laser application technology, Springer, 2011. 343-349

[7] Li, Z.; Wang, J. Wu, Q. (2012) Ultrashort pulsed laser micromachining of polycrystalline diamond. In: Advanced Materials Research Vol. 497 p. 220-224

[8] Li, Z.; Wang, J.; Wu, Q. (2012) Molecular dynamics simulation of the ablation process in ultrashort pulsed laser machining of polycrystalline diamond. In: Advanced Materials Research Vol. 500, pp. 351-356

[9] Westraadt, J.E.; Dubrovinskaia, N.; Neethling, J.H.; Sigalas, I. (2007) Thermally stable polycrystalline diamond sintered with calcium carbonate. In: Diamond & Related Materials 16, 1929–1935

[10] Weikert, M. (2005) Oberflächenstrukturieren mit ultrakurzen Laserpulsen. In: Laser in der Materialbearbeitung, Forschungsberichte des IFSW. Herbert Utz Verlag, München, . p. 33ff.

[11] Biermann, D.; Würz, E. (2009) A study of grinding silicon nitride and cemented carbide materials with diamond grinding wheels, Production Engineering Research and Development, Vol. 3

[12] Friemuth, T. (2002) Herstellung spanender Werkzeuge, Universität Hannover, Habilitation

[13] Kenter, M. (1990) Schleifen von polykristallinem Diamant, Universität Bremen, Dissertation

[14] C. Michels: Nur mit optimalem System Schleifen von CBN-/PKD-Werkzeugen, VDI-Z Special Werkzeuge, 2003

[15] L. Pastewka; S. Moser: Anisotropic mechanical amorphization drives wear in diamond, Nature Materials Volume 10, 2011

[16] F. Klocke: Manufacturing Processes II, Grinding, Honing, Lapping, Springer, 2008

[17] A. Y-C. Yu, T.M. Donovan, W.E. Spicer: Optical properties of cobalt. In: Physical Review Vol. 167 No. 3, 1968, p. 670-673

[18] C. Dold et al.: Comparison of ground and laser machined polycrystalline diamond (PCD) tools in cutting carbon fiber reinforced plastics (CFRP) for aircraft structures, Procedia CIRP, Volume 1, p 178, 2012